IEEE Access
Multidisciplinary | Rapid Review | Open Access Journal

Received November 9, 2020, accepted November 15, 2020, date of publication November 18, 2020,
date of current version December 3, 2020.

Digital Object Identifier 10.1109/ACCESS.2020.3038917

An Indoor Global Localization Technique for Mobile Robots in Long Straight Environments

LINGDONG ZENG[1], (Graduate Student Member, IEEE), SHUAI GUO[1,2], ZHEN XU[1], AND MENGMENG ZHU[1]

[1]Shanghai Key Laboratory of Intelligent Manufacturing and Robotics, School of Mechatronic Engineering and Automation, Shanghai University, Shanghai 201900, China
[2]Shanghai Robot Industrial Technology Research Institute, Shanghai 200062, China

Corresponding author: Shuai Guo (guoshuai@shu.edu.cn)

This work was supported by the National Natural Science Foundation of China under Grant U1913603.

ABSTRACT Scan matching methods have been widely applied in the fields of autonomous localization and mapping. However, in structured environments where feature differences are less significant, such as long straight corridors, conventional positioning algorithms often suffer from characteristic mismatching, resulting in lower accuracy. As such, a new global localization algorithm, based on environmental difference evaluation and correlation scan matching fusion, is proposed in this study. In this process, the surrounding space was evaluated using a priori understanding of the environment based on a linear fit. Corresponding evaluation and positioning results from correlation scan matching were then modified using dynamic selection and a posture updating strategy. The performance of the proposed technique was compared with other conventional methods using open datasets exhibiting long straight features and a series of tests conducted in a physical corridor. Results showed that the proposed algorithm could effectively improve localization accuracy in narrow environments. The translation and rotation absolute pose errors were reduced by an average of 27.29% and 25.82%, respectively, compared with a correlation matching approach that does not consider the surrounding geometry. These results suggest the proposed technique offers higher adaptability and positioning accuracy in narrow environments.

INDEX TERMS Environmental characteristics, global localization, line fitting, mobile robot, scan matching.

I. INTRODUCTION

The simultaneous localization and mapping (SLAM) building problem involves placing a mobile robot in an unknown starting location in an unfamiliar environment. The robot must then incrementally construct a map of this environment while simultaneously using this map to calculate its absolute location [1]–[3]. Mobile robots can output their current position quickly and accurately using an existing map and the surrounding environment, which are critical for the subsequent realization of path planning, obstacle avoidance, and other functions. It is also more practical to track the pose of a robot against a known map, which could be constructed from the workspace of other mobile robots.

In recent years, the scanning matching global localization method, based on 2D laser input data, has played an important role in the positioning of mobile robots. Scan matching seeks a set of translation and rotation parameters to maximize the overlap of two scanned point clouds after alignment [4]–[6].Two or more consecutive scanned laser point clouds can then be unified in the same coordinate system, by solving for the coordinate transformation relationship. The current scanned point cloud can also be registered with an established map to recover changes in robot body posture. This process is illustrated in Figure 1.

Existing scan matching techniques can be divided into three categories: point-based, mathematical feature-based, and likelihood field estimation-based algorithms. The iterative closest point (ICP) model and its variations represent point-based scan matching algorithms, which are also more sophisticated approaches. In this process, the basic model is provided with a scanning point cloud and a reference point cloud for current laser data. These are used to solve the rigid body transformation matrix and minimize the Euclidean distance for corresponding points [7], [8]. The most representative scanning matching based on mathematical features is the

The associate editor coordinating the review of this manuscript and approving it for publication was Hui Xie.

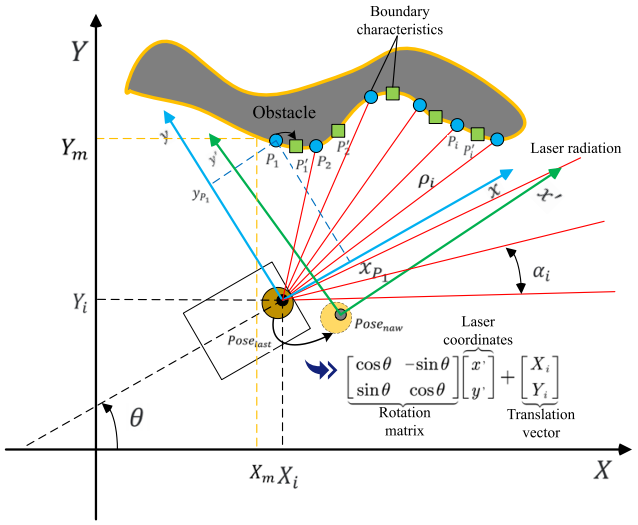

FIGURE 1. A scanning matching technique based on 2D lidar, in which the relative transformation relationship between poses is determined in the same coordinate system.

normal distribution transform (NDT), which maps discrete 2D points from a single scan into a segmented continuous and differentiable probability density, defined on a two-dimensional plane [9], [10]. The scan matching method based on the likelihood field estimation constructs a likelihood field using existing grids. It then specifies the search space, calculates a score for each pose in the search space, and determines the variance of a match using the pose score. Correlation scan matching (CSM) is an application of the likelihood field raster technique [11]–[13]. The primary advantage of this approach is that current scan data and multi-scan historical data can be used to improve matching accuracy. Global optimization can then be ensured through grid division. However, in the case of small environmental differences, such as long straight corridors, depth information acquired by a laser rangefinder does not change significantly with time, which complicates attitude estimation [14], [15].

Scan matching algorithms typically do not consider the effects of long straight environments on localization accuracy. This is particularly true for conventional CSM algorithms that require the use of adjacent likelihood regions and boundary features for registration. However, long-term corridor features do not include enough information to estimate complete poses, which results in fewer matches and larger positioning errors. Environments with linear and planar structures, such as offices and factories, often contain large numbers of long and straight spaces. These natural features should be considered to improve positioning accuracy for industrial applications [16], [17].

This study presents novel a localization technique suitable for long and straight indoor environments. The approach fully considers the characteristics of such spaces and evaluates the corresponding geometry with a line-fitting algorithm. A priori understanding of the current robot environment was acquired using line fitting. The localization results exhibit varying dependence on the dynamic selection of a robot posture updating strategy. The contributions of this work focus primarily on the following three points:

1) A prior understanding of the robot's current environment is critical for global positioning in long straight corridors. This study proposes a new methodology for evaluating the characteristics of long straight environments, based on linear fitting, using only laser sensors.
2) In long corridors with no obvious textural features, global positioning based on scan matching lacks forward and backward constraints, preventing a robot from perceiving its own X direction coordinates and causing position drift. To solve this problem, correlation scan matching algorithms and line fitting were combined in this study, to develop a more accurate global localization result for narrow corridor environments.
3) The method proposed in this article was tested in both virtual and physical environments. Tests performed using a public data set showed this method is more robust than ICP or combined RANSAC and more accurate for judgments in long straight environments. Test results in physical environments showed improved reliability in static corridors.

The remainder of this article is organized as follows. A description of related work is provided in Section 2. Theoretical definitions, derivations, and the environmental detection algorithm workflow for 2D laser scanning matching are included in Section 3. A validation experiment is then conducted, and the results are analyzed in Section 4. Section 5 concludes this article.

II. RELATED WORKS

This section summarizes existing 2D laser scan matching methods and related line fitting models. Some of the most relevant and recent works are discussed, including point scan matching, mathematical feature scan matching, and likelihood field scan matching. A brief review of line fitting is also included.

A. SCAN MATCHING

Scan matching is a common technique for registering laser data acquired in different poses and determining relative pose transformations. The laser source is used to scan a flat object surface at a fixed angular resolution α_i, returning several successive measurements $\{\rho_i | \cdots \rho_{i-1}, \rho_i, \rho_{i+1} \cdots\}$. The values of laser scanning points in the coordinate system of the mobile robot can then be determined from the angular resolution and distance measured by the laser. The position of the mobile robot in the global coordinate system can be acquired through a coordinate transformation, using the relationship between the current position and the next position, represented by(X_i, Y_i, θ). Scan matching was typically conducted using ICP and its variations, NDT or CSM.

ICP is a popular optimal registration algorithm based on the least-squares method. In this process, corresponding

relational point pairs are selected repeatedly for two sets of laser-point cloud data with similar local geometric features. An optimal rigid body transformation is then calculated until the convergence requirements for accurate registration are met [18], [19]. Zhu *et al.* proposed an indoor robot-positioning model based on ICP scan matching, which was used to modify a robot motion model and reduce the uncertainty of robot attitude in the prediction step [20]. Censi described an ICP variation using point-to-line metrics and a precise closed-form that minimized the corresponding metrics [21]. Pavlov *et al.* [22] proposed a new methodology for accelerating ICP, based on the Anderson acceleration technique. This algorithm is typically faster than the standard Picard iterative method. Although ICP can achieve high accuracy in scan matching, its strong dependence on the quality of initial data associations reduces its applicability in practical applications. In addition, its computational efficiency and robustness need to be improved further [23], [24].

In addition to ICP-based models, scan matching methods such as NDT use mathematical properties to characterize data and inter-frame pose changes. Biber and Strasser applied NDT to laser scan matching between frames, defining a score for the probability density after registration [9], Li *et al.* addressed the difficulty of extracting typical features in unstructured rescue environments, using NDT scan matching to estimate probability distributions for laser data. Their proposed NDT-EKF algorithm combined NDT scan matching with the EKF framework [25]. He *et al.* used NDT to match the current keyframe with a local map and construct a new map at a lower frequency [26].

Both ICP and NDT exhibit certain requirements for initial values. As such, correlation based on exhaustive matching performs well in a variety of settings. Olson described a matching algorithm based on the correlation of two lidar scans. This approach resolved the issue in a probabilistic framework and identified a rigid-body transformation that maximized the probability for observed data [12], Olson also developed a new multi-resolution scan matching approach that makes exhaustive matching practical, even for large positional uncertainties [11]. Hess *et al.* combined branch definition algorithms to increase search efficiency based on CSM scan matching [27]. Song *et al.* introduced a global localization strategy for 2D laser ranging robots, based on depth-first searches and grid diagrams [13].

Scanning matching, a common positioning technique, has been used in a variety of studies that rely on external sensors. For example, Yuxiang *et al.* developed an indoor positioning system, based on Wi-Fi signal strength, and implemented a fingerprint matching algorithm derived from the improved KNN algorithm and Gaussian process regression [28]. Codas *et al.* proposed a localization model based on a particle filter, by integrating RFID sensors and odometers [29]. This algorithm successfully localized a mobile robot with bounded error estimation, while dead reckoning approaches using only odometry caused the error to diverge. Relying solely on an odometer during global positioning will lead to the accumulation of positioning errors and inaccurate results. Martin *et al.* leveraged recent advances in deep learning and variational inference to correct dynamical and observation models for state-space systems [30]. This approach trains Gaussian processes on the residuals between the original model and the ground truth, and has been applied to publicly available datasets for robot navigation based on two-wheel encoders, a fiber optic gyro, and an inertial measurement unit.

Most location techniques using external sensors require changing the existing environment, which is often impractical. In addition, odometer-based dead-reckoning positioning models calculate new position values using only the value derived in the previous step. As a result, the error and uncertainty of position estimation are cumulative and increase with time. Requiring odometers to coordinate with other sensors, such as an RFID [29], reduces the integrity of the environment. In other words, before the positioning process can occur, the corresponding sensing equipment must be assembled in the environment where the robot is to be located.

The primary goal of this article is the realization of robot positioning in long straight corridors, based on scanning matching, without changing the environmental state. Both ICP and NDT models depend heavily on the initial pose, which can easily lead to local minima. The primary advantage of the CSM method is that current-frame laser data and multi-frame historical data are used to improve the accuracy of probability matching, which can maintain global optimums in raster divisions. However, CSM is prone to mismatching when environmental differences are small [17]. These salient features should be considered for global localization in artificial environments composed of linear features, such as homes, offices, and factories [16].

B. LINE EXTRACTION

A line extraction model, based on 2D laser data, was found to be the most useful in describing the long and straight characteristics of corridor environments. Several different line extraction algorithms have been proposed in recent years. Only basic versions of these algorithms are discussed here, chosen for their performance and popularity in mobile robotics and feature extraction.

Borges proposed a segmentation method for line extraction in 2D range images [31], This model has been used for mobile robot navigation systems and dynamic map building. Zhang *et al.* used the split-and-merge technique for map building and described localization techniques for a mobile robot equipped with a 2D laser rangefinder [32]. Schaefer at el. used a novel probabilistic method to extract polylines from raw 2D laser data [16], The goal of this approach was to determine a set of polylines that maximized the likelihood of a given scan. Gao *et al.* proposed a line segment extraction algorithm, using laser data, based on seeded region growing [33]. RANSAC has been used to roughly estimate 3D transformations by finding an optimum consensus

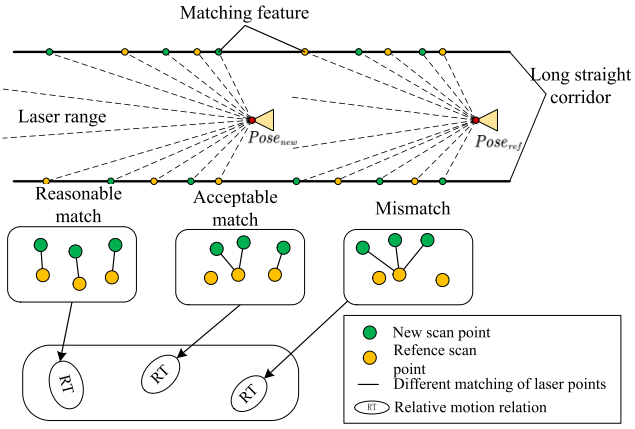

FIGURE 2. A schematic diagram of laser point mismatching in long straight corridors. The relative motion estimation errors were caused by laser point mismatching, which led to a decrease in global localization accuracy.

model [34], a common linear fitting method. This algorithm has also been used for robust fitting of models in the presence of data outliers. The primary advantage of RANSAC is its robustness as a generic segmentation method that can be used with several types of features once the feature model is determined [35]. Samuel *et al.* proposed a weighted line-fitting technique that weights the influence of each point on a fit, according to its uncertainty, which can be derived from sensor noise models [36].A key feature and contribution of this method is the concrete formula for the covariance of the line segment fitting while allowing for individual weighting of each measured point. Therefore, we use the weighted line extraction method to describe the long straight corridor environment.

C. PROBLEM STATEMENT

Although a variety of scan matching and line extraction techniques have been proposed and implemented, it is still necessary to improve global localization accuracy in narrow corridor environments. When a mobile robot is in this type of environment, with no other references, the input of two laser beams returns the same scan point. As a result, the matching algorithm returns the same score at all locations in the mapped area. The region where the mobile robot is located can then not be correctly matched, regardless of whether a scan line is added or not. As shown in Figure 2, $Pose_{new}$ can be acquired from $Pose_{new} = Pose_{ref} \otimes RT$, where RT represents the relative rotation and translation relationship between $Pose_{new}$ and $Pose_{ref}$. The term $\otimes$ represents a combination of the coordinate systems.

The single geometric structure of long corridors results in a loss of forward and backward constraints in current LiDAR SLAM techniques when point cloud matching is done at the front end. This prevents the robot from perceiving its own X direction coordinates in the corridor, causing position drift. Misjudging the correlation of any laser point in the two beams, while leaving the correlation of other points unchanged, will produce a new correlation configuration that differs from the ideal value. As in visual SLAM, incorrect data associations can lead to catastrophic failures in the localization processes [37]. An incorrect global pose relationship RT will then reduce the accuracy of a pose. As such, this study attempts to improve global localization accuracy for mobile robots in narrow environments. Line extraction is adopted to evaluate these straight environments and the dependence of scan matching results on the dynamic selection of a robot posture updating strategy is investigated.

III. METHODOLOGY

In narrow environments, it is necessary to determine geometric characteristics using line extraction. Scans can then be used to match the output global poses. An overview of the proposed approach is shown in Figure 3. The framework can be divided into three steps: scanning matching, environment evaluation, and pose fusion. Scanning matching included the most popular correlation scanning matching algorithms. Environmental assessment included linear fitting and difference assessment methods. Pose fusion occurred after environmental assessment. The global localization problem based on scan matching can then be described as follows. The same map features are observed at different times to acquire rotation and translation changes for the posture of the robot between adjacent frames.

A. CORRELATIVE SCAN MATCHING

Unlike the NDT and ICP algorithms that depend heavily on initial pose, correlation scan matching is robust to large initialization errors. The target of the CSM is defined by starting a search from the previous pose frame and finding an optimal pose transformation, such that the position of the scan point in the map corresponds to the grid with the largest possible degree of occupation. This approach utilizes a probabilistic framework to search for a rigid transformation that maximizes the probability of having the observed data.

Global localization based on scan matching can be defined as the prediction of trajectories under the conditions of a known map. The probability model can be described as $p(x_t|x_{t-1}, m_{t-1}, z_t, u_{t-1})$ and used to estimate the robot position at time t, given the robot position map m_{t-1}, a control u_{t-1} at the previous instance, and the observation z_t at the current instance. In this context, Bayes rule can be expressed as:

$$p(x_t|x_{t-1}, m_{t-1}, z_t, u_{t-1}) = \frac{p(z_t|x_t, m_{1:t-1})p(x_t|x_{t-1}, u_t)}{p(z_t|x_{1:t-1}, m_{1:t-1})} \tag{1}$$

Since the sample weight factor in $p(z_t|x_{1:t-1}, m_{1:t-1})$will be normalized to 1, and is independent of $x_t$it will be canceled in the process of algorithm standardization. As such, no calculation is required.

$$p(x_t|x_{t-1}, m_{t-1}, z_t, u_{t-1}) \propto p(z_t|x_t, m_{1:t-1})p(x_t|x_{t-1}, u_t) \tag{2}$$

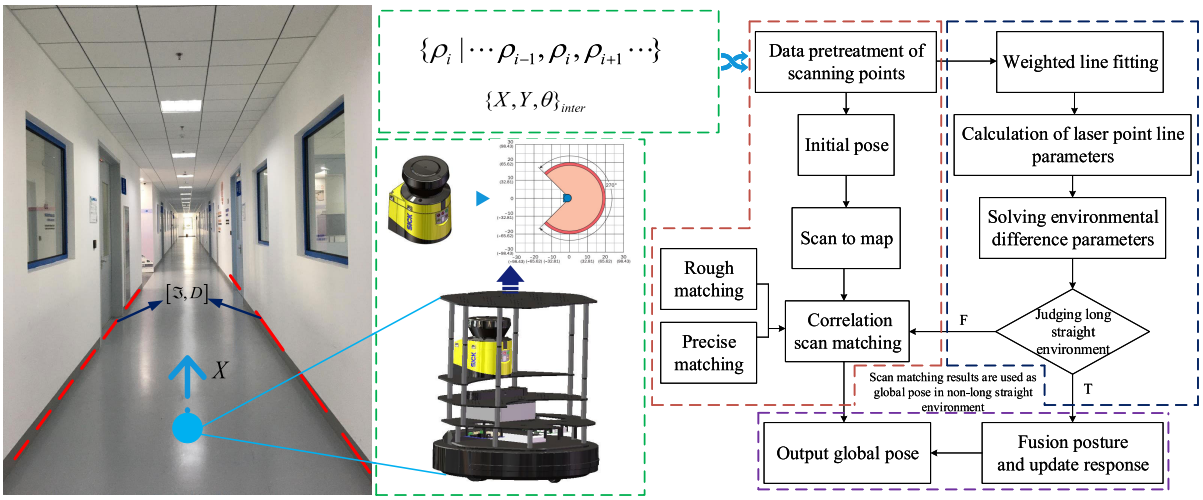

FIGURE 3. The proposed indoor global localization framework for mobile robots in long straight environments.

The term $p(x_t|x_{t-1}, u_t)$ can be acquired using IMU and an odometer. The observation model $p(z_t|x_t, m_{1:t-1})$ then becomes the primary focus of algorithm development. Each lidar scanning observation z_t is independent of the others. As such, the observation model can be described as:

$$p(z|x_t, m) = \prod_i p(z_i|x_t, m) \tag{3}$$

The proposed global localization is based on a calculation of maximum likelihood estimation for $p(z|x_t, m)$ Therefore, equation (3) can be used to express the problem as [38]:

$$\begin{aligned} \hat{x}_t &= arg\max_{x_t} \prod_i p(z_i|x_t, m) \\ &= arg\min_{x_t} \prod_i -\ln p(z_i|x_t, m) \\ &= arg\max_{x_t} \sum_i \ln p(x_i(z_i)|m_{grid}) \end{aligned} \tag{4}$$

where $\hat{x}_t$ is the final output pose, while m_{grid} represents known map. Accurately defining this term is the primary goal of maximum likelihood estimation in the proposed algorithm. The matching and positioning processes for known maps involves outputting a transformation relationship for the coordinate system of the mobile robot, when the laser in the current frame is aligned with the point cloud in the map.

The optimal rigidity transformation is assumed to be $\hat{x}_t = (\Delta x, \Delta y, \varphi)$. The position of the radar point after a rigidity update can then be expressed as:

$$G(\hat{x}) = \begin{bmatrix} \cos\varphi & -\sin\varphi \\ \sin\varphi & \cos\varphi \end{bmatrix} \begin{bmatrix} G_{t,x} \\ G_{t,y} \end{bmatrix} + \begin{bmatrix} \Delta x \\ \Delta y \end{bmatrix} \tag{5}$$

The process of identifying an optimal rigid transformation can be understood as searching for all possible pose orientations in a search interval, then scoring the results. The pose with the highest score represents the current optimal transformation result, as shown in Figure 4. The process

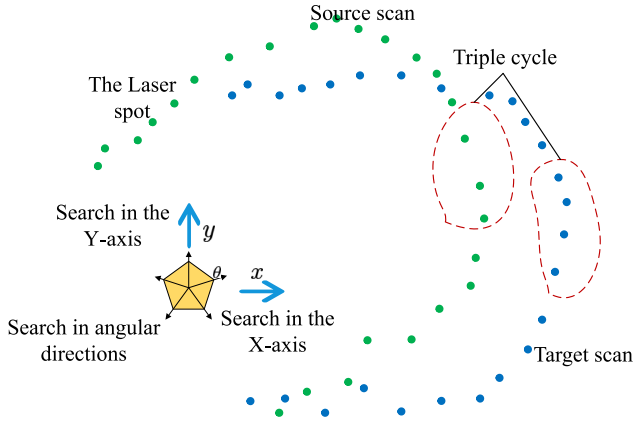

FIGURE 4. The process of exhaustive matching, the angular directions, the *X* axis, and the *Y* axis of the triple cycle, matching the optimal pose. When the best registration is found, the translation and rotation will be output.

for high-resolution matching scores is consistent with that of low-resolution scores. Finally, the optimal conversion is output for the score with the highest match.

The conventional multi-resolution CSM model is described in Algorithm 1 [11], [12], [27]. The required input includes a grid map (to be located) and current laser data, as well as a fuzzy value representing the initial pose. The output is a transformation relationship developed from the optimal matching score. The input laser data are initially rasterized and blurred using a Gaussian kernel. Each raster is then assigned a score based on the mapping results. Exhaustive matching is then conducted and the score is calculated for θ, x, and y.

The third line of Algorithm 1 is the Gaussian smear process. If a grid coordinate is selected by a laser scan, the surrounding grids will also be assigned according to a Gaussian distribution (the correlation step). Lines 4-9 and 10-15 are two exhaustive-search matching processes with differing grid

Algorithm 1: The Correlation Scan Matching Algorithm

Input: Target scan m_{grid}, Source scan z_i, Initial transform $\hat{x}_0$
Output: Optimal rigidity transformation $\hat{x}$, Scan matching score S_H^{best}

Initialization of scan matching score: $S_L^{best} \leftarrow 0, S_H^{best} \leftarrow 0$
Laser data projection with certain angle resolution: $m_{subgrid}^{low} \leftarrow z_i^{t_i}, m_{subgrid}^{high} \leftarrow z_i^{t_i}$
Gaussian smear grid: $m_{subgrid}^{low} \leftarrow e^{-\frac{x^2+y^2}{2\sigma^2}}$
for *i =1 to N* **do**
  $S_L^i \leftarrow \sum_{k=1}^{m} m_{subgrid}^{low}(\Delta\hat{x}_t^i \hat{x}_L^* z_i^{t_i})$
  if $S_L^i > S_L^{best}$ **then**
    $S_L^{best} \leftarrow S_L^i, \hat{x}_L^* \leftarrow \hat{x}_t^i$
  end
end
for *i =1 to M* **do**
  $S_H^i \leftarrow \sum_{k=1}^{m} m_{subgrid}^{high}(\Delta\hat{x}_t^i \hat{x}_H^* z_i^{t_i})$
  if $S_H^i > S_H^{best}$ **then**
    $S_H^{best} \leftarrow S_H^i, \hat{x}_H^* \leftarrow \hat{x}_t^i$
  end
end
$\hat{x} \leftarrow \hat{x}_H^*$
Return $\hat{x}, \hat{x}_H^{best}$

precisions. The final output is the optimal pose transformation in the laser coordinate system and the corresponding matching score.

B. LINE EXTRACTION FOR ENVIRONMENTAL EVALUATION

Man-made environments such as houses, offices, or factory floors are typically composed of linear structures. As such, line extraction was used to evaluate flat surfaces in narrow spaces, distinguishing their geometries from similar structures for scan-matching positioning in complex environments.

In this study, the straightness of an object was described by the slope of a fitted line and the length of the object was represented by the length of the line segment. Weighted line fitting is a common 2D line extraction algorithm based on expectation maximization [31]. This approach weights the influence of each point on the overall fit, according to its uncertainty derived from sensor noise models. The robot moves through multiple poses where are represented by (X_i, Y_i, θ). A frame of laser scan contains fixed angular resolution α_i and several successive measurements ρ_i. the measured distance to the environment's boundary in the direction denoted by β_i. Generally, ρ_i be comprised of the true range and additive noise term. At each pose, the robot gathers a range scan and the scan point coordinates are described in the laser coordinate frame:

$$u_i = (\rho_i + \varepsilon_\rho)\begin{bmatrix}\cos(\beta_i + \varepsilon_\beta)\\ \sin(\beta_i + \varepsilon_\beta)\end{bmatrix} \tag{6}$$

where ε_ρ and ε_β are considered the distance noise and angle noise, respectively, which are assumed to be a zero-mean Gaussian. The noise model for the sensor uses a maximum likelihood approach to formulate a general strategy for estimating the line of best fit from a set of non-uniformly weighted range measurements. This process is shown in Algorithm 2 below.

Algorithm 2: The Weighted Line Fitting Algorithm

Input: The points of the scan N_p
Output: The line model paraments

Initialization of points of the scan: N_p
for *i to* N_p **do**
  Initial random estimation generates line parameters
  Initializes the weight of the remaining points
  for *j to* $(N_p - i)$ **do**
    Compute the weights of the points from the line model
    Recompute the line model parameters
    Max.N.Steps reached or convergence
  end
  Max.N.Trials reached or found a line
end
if *the line model paraments exist* **then**
  store the line, remove the inliers, go to step2
  else
    Terminate
  end
end

Linear parameters were generated randomly from the laser data and weights for the remaining points were calculated using the linear model, until the maximum number of iteration steps or convergence was reached. The complexity of this algorithm is low and, as shown in Figure 5, it was replicated in TurtleBot2 with SICK LMS111.

However, fitting a line segment to the 2D laser data is not the primary goal. The collected data were used not only for scan-matching positioning but also for subscription during the fitting process. Our objective was to evaluate the environment encountered by the mobile robot using these linear parameters.

The slopes k_1 and k_2 for segments L_1 and L_2 were calculated by line fitting, as shown in Figure 6. The values of k_1 and k_2 determined how the environment was classified (i.e., long straight), as follows:

$$\Im = \sin\psi = \left|\frac{k_1 - k_2}{1 + k_1 k_2}\right| \sqrt{(1 + (\frac{k_1 - k_2}{1 + k_1 k_2})^{\,2})^{-1}} \tag{7}$$

The term $\Im$ was used to quantify varying degrees of environmental properties and distinguish narrow structures from

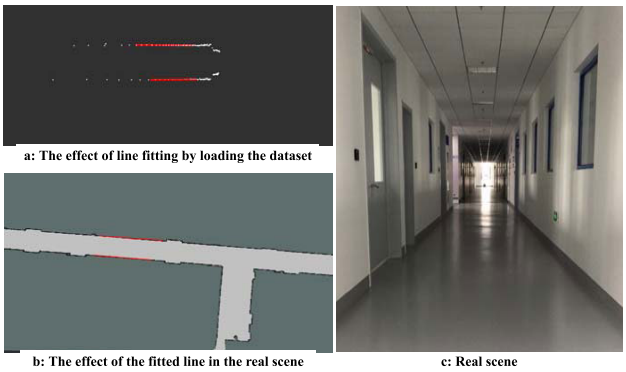

FIGURE 5. Weighted line-fitting results. The white markers are laser points and the red markers represent the fitted line coordinates. Also shown are: a) the effect of line fitting by loading the dataset, b) the effect of the fitted line in the real scene, and c) real scene.

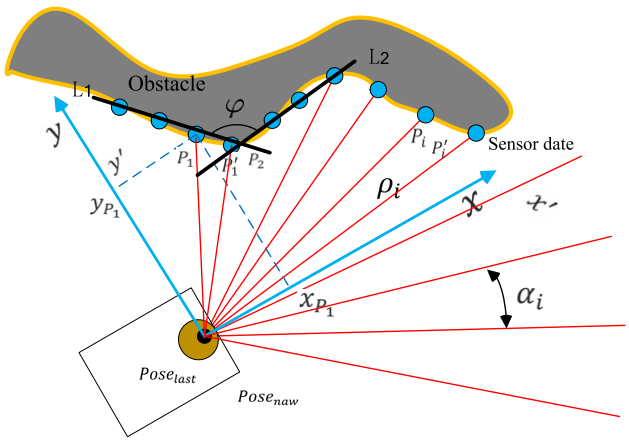

FIGURE 6. The fitted line segment in the laser coordinate system. The angle between the two adjacent lines can be calculated according to the parameters of the line segment and used to evaluate the environment.

the general background. When $\Im$ was close to 1 and ψ was close to $\pi/2$, differences in sample points were obvious and the environment was not considered straight. When $\Im$ was close to 0 and ψ was close to π, the corresponding structure was assumed to be long and straight. As such, the mobile robot is instructed to process the location results from scanning matching.

The results of line fitting may correspond to continuous short lines, in which case the environmental characteristics are relatively evident and superior positioning information can be acquired with CSM. In addition to the angle threshold, we must also consider the distance threshold. The distance s between a fixed point on the fitted lines (P_i) and either of the endpoints (P_{i-1} or P_{i+1}) can be expressed as:

$$s = \sqrt{(P_{i-1,y} - P_{i,y})^2 + (P_{i-1,x} - P_{i,x})^2} \tag{8}$$

The angular threshold can then be defined as:

$$D = s\Im \tag{9}$$

A value of D that is smaller than $\Im$ indicates the fitting line to be a continuous short line, representing a rapidly changing environment.

C. GLOBAL LOCALIZATION ALGORITHM CONSIDERING LONG AND STRAIGHT ENVIRONMENT

In the case of narrow environments, an improved global location can be acquired through the evaluation of environmental differences, using line fitting and CSM-based scanning matching.

Algorithm 3: Global Localization Algorithm for the Long Straight Environment

Input: maps, readings ς, d, t
Output: Position (X, Y, θ)
Initialization of *maps, readings*, ς, d, t
$[k_I, k_{I-1}] \leftarrow$ Weighted line fitting *(readings)*
$[\Im, D] \leftarrow [k_I, k_{I-1}]$
if $[\Im, D] > [\varsigma, d]$ **then**
  maps $\leftarrow$ *readings*
  for $n_{x,y} = 0 : n$ **do**
    for $n_\theta = 0 : 4$ **do**
      $S^i \leftarrow \sum_{k=1}^{m} m^{high}_{subgrid}(\Delta\hat{x}^i_l \hat{x}^* z^{t_i}_i)$
    end
  end
  Position(X, Y, θ)
end
else
  $(X, Y, \theta) = p(X, Y, \theta)_{csm} + (1-p)(X, Y, \theta)_{inter}$
end
Calculate (X, Y, θ)

In the previous section, angular and distance parameters were acquired and threshold values were set according to empirical results. For example, when the degree of environmental difference is small, environmental similarity is high. The global pose value acquired after CSM matching is then introduced into the odometer and internal sensor to produce a joint global pose in the laser frame for P_i, This process can be described as:

$$(X, Y, \theta) = p(X, Y, \theta)_{csm} + (1-p)(X, Y, \theta)_{inter} \tag{10}$$

where p represents the influence of environmental similarity on positioning results. This is an empirical threshold, considered to be variable depending on the situation. The dependence of scan matching results on the dynamic selection of a robot posture updating strategy was investigated using environment information from the previous position. This global localization method considering environmental diversity is represented in Algorithm 3.

This algorithm first develops a priori understanding of the environment through line extraction and then provides the corresponding global pose through CSM.

TABLE 1. Different Standard Datasets and Characteristics.

Name	Laser frames	Output pose number	Long straight environment
ACES-Building	7374	1543	Yes
MIT-Killian-Court	87400	6268	Yes

IV. VERIFICATION AND EXPERIMENTS

The proposed algorithm was evaluated through a series of experiments. The assessment metrics for global positioning errors are first introduced and the algorithm is then tested using a public data set. Finally, the model was tested in a physical environment using a mobile robot in a long straight corridor. The results from each experiment are then presented and discussed.

A. EVALUATION OF ERROR MEASUREMENT

In some instances, the accurate and inaccurate positioning results could be distinguished visually, through a mapping effect. However, as algorithm performance improved and the amount of data increased, direct observational evaluation became increasingly poor. The evaluation methodology used in this experiment can be described as follows. Root mean square error (RMSE) and relative pose error (RPE) are common evaluation metrics in SLAM applications [39]–[42].

RMSE measures the mean deviation between an estimated value and the correct value. In 2D laser-based SLAM problems, two different RMSE measurements are needed to represent errors in both translation and rotation. Although RMSE is not particularly useful for rotation errors, translation errors in narrow environments are far more prevalent. As such, RMSE was used as the primary evaluation metric for the algorithm proposed in this study. The errors in 2D translations can be defined as:

$$RMSE_{pos_{tra}} = \sqrt{\frac{1}{n}\sum_{i}^{n}(x_i^{x,y} - \hat{x}_i^{x,y})^2} \tag{11}$$

The rotational component of RMSE is then given by:

$$RMSE_{pos_{rot}} = \sqrt{\frac{1}{n}\sum_{i}^{n}(x_i^{\theta} - \hat{x}_i^{\theta})^2} \tag{12}$$

where $x_i^{x,y} = (x_i, y_i)^T$ represents the estimated robot position and $\hat{x}_i^{x,y}$ indicates the actual robot position.

B. VALIDATION ON DATASETS

Two different standard datasets, listed in Table 1, were used to evaluate the proposed algorithm. The map created with each dataset is shown in Figure 7. It is evident from the figure that these sets include data from a large number of long and straight corridors. It is also clear that global localization based on scan matching is prone to inaccurate positioning, due to the high similarity of relevant characteristics.

As such, five regions constructed from two datasets (ACES-Building and MIT-Killian-Court) were selected from the map and compared with the parameters of lines fitted in each region. This type of line extraction was used to develop an initial description of the environment.

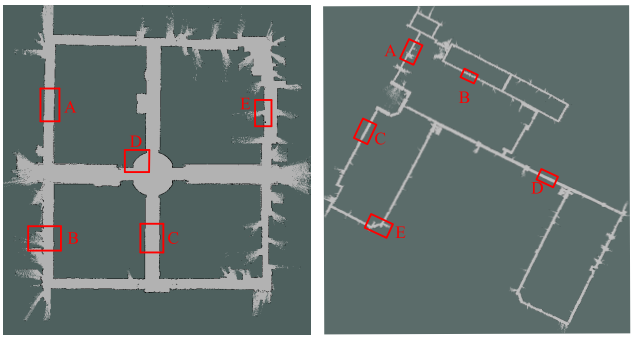

a: ACES-Building b: MIT-Killian-Court

FIGURE 7. Maps from the a) ACES-Building and b) MIT-Killian-Court datasets, which contain several long straight elements. The area selected by the red box is the region corresponding pose number.

TABLE 2. The Lengths and Angles Corresponing to The Five Regions of The ACES-Buliding Dataset.

Regions	Corresponding pose number	Angle (°)	Length (m)
A	122	0.75804	5.34076
B	985	-7.6604	3.75576
C	1217	8.0946	5.57053
D	1007	-34.4468	0.98299
E	446	62.9838	2.46244

TABLE 3. The Lengths and Angles Corresponing to The Five Regions of The MIT-Killian-Court Dataset.

Regions	Corresponding pose number	Angle (°)	Length (m)
A	178	2.67514	4.0704
B	927	-0.156111	7.0529
C	3894	-1.30528	6.2457
D	4184	-3.10137	5.0199
E	4738	38.6834	1.3328

However, each region may contain multiple corresponding pose numbers. For this reason, the length and angle corresponding to a pose in the middle of the region were selected as representatives of the region (see Tables 2 and 3).

The angle in these tables was measured in the laser coordinate system, where small angles indicate segments are approximately parallel to the *Y-axis*, while angles approaching 90° indicate the segments are nearly parallel to the *X-axis*. The length refers to the magnitude of the fitted line segment. As seen in Figure 7, these line segments were shorter, with an angle between 0° and 90°, in non-straight environments. Conversely, fitted line lengths were longer and the angles were closer to 0° or 90° in long straight environments. This suggests that line fitting plays a descriptive role in environment classification.

The ACES-Building and MIT-Killian-Court datasets were collected in real environments, making it difficult to acquire accurate absolute motion information. As such, the optimized global pose approximation (with loop optimization) was used as the real value [43]. Three different pose trajectories are

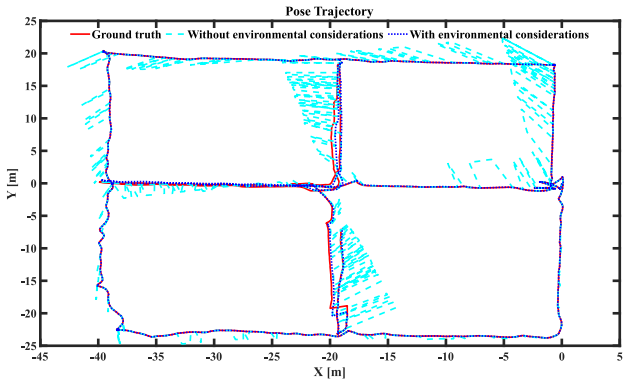

FIGURE 8. Posture trajectory tracking of the ACES-Building. The red polyline is the ground truth that obtained by loop optimization, while the blue polyline and the indigo polyline are pose trajectories without considering environmental factors and with the environment factors respectively.

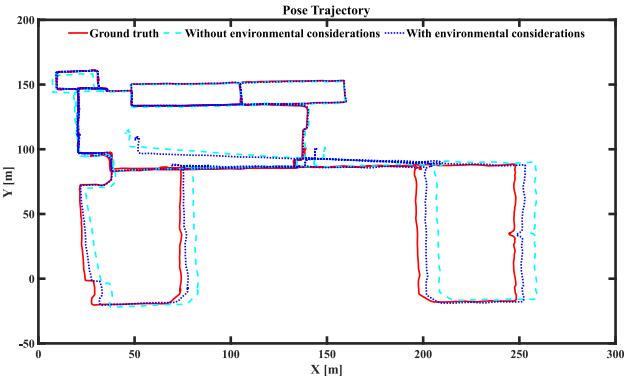

FIGURE 9. Posture trajectory tracking of the MIT-Killian-Court. The red polyline is the ground truth, the blue polyline and the indigo polyline are posture trajectories without considering environmental factors and with the environment factors respectively.

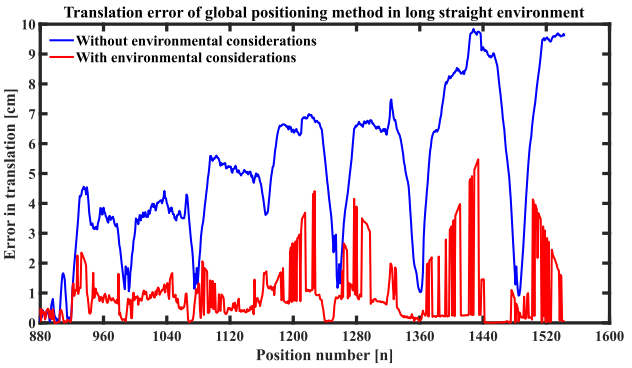

FIGURE 10. Translation error of the ACES-Building. The blue polyline is the mean square error without considering the influence of long straight environmental parameters, while the red polyline is the mean square error with considering the influence.

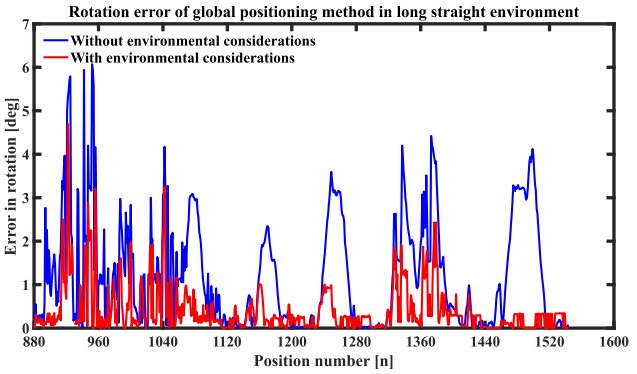

FIGURE 11. Rotation error of the ACES-Building. The blue polyline is the mean square error without considering the influence of long straight environmental parameters, while the red polyline is the mean square error with considering the influence.

given first in Fig.8 and Fig.9. The mean square error of this global pose, with and without consideration of the straight environment, was then calculated.

It can be seen from the pose trajectory map that the pose without considering the long and straight characteristics of the environment exhibit high noise. In addition, the pose trajectory considering environmental factors coincides nicely with the assumed true value, which also indicates that environmental factors have a positive impact on positioning results.

Both ACES-Building and MIT-Killian-Court dataset contain a large number of long and straight environment features, and MIT-Killian-Court dataset scenario is much larger than ACES-Building dataset scenario. Although it is not in perfect agreement with the results of laser tracking, the pose trajectory produced by considering the characteristics of the long straight corridor is closer to the true value than the trajectory produced without environmental considerations. This was particularly true for large scenes, as is evident in Fig. 9.

Figures 10 and 11 respectively show the translation and rotation absolute pose errors produced by considering the influence of narrow environment characteristics for the ACES-Building dataset. The abscissa represents the number of positions, while the ordinate is an indication of the degree of error.

Loop optimization requires the loop to be checked before correcting the pose. However, no loop was detected prior to an *X-axis* value of 880. In other words, the approximate true value of the pose was the same as the value without optimization. As such, the decision of whether to consider the influence of long straight environments in global pose estimation is negligible.

However, it does not affect the evaluation of the experiment, after the first loop point ($x = 880$), it is easy to acquire a global pose that considers environmental influences, which offer more accurate positioning results. It can be seen from the figure that the method considering the characteristics of environment length and straightness achieved superior global positioning performance as measured by both translation and rotation absolute pose error.

The MIT-Killian-Court dataset is composed of infinite corridors, which are especially suitable for testing the proposed model. the differences between rotation and translation errors for models that do and do not consider the influence of

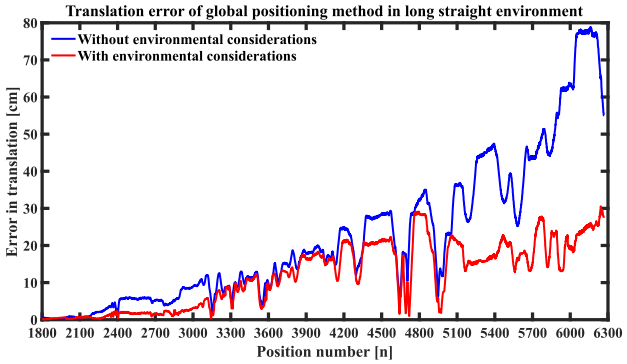

FIGURE 12. Translation error of the MIT-Killian-Court. The long-term large environment makes the error value in the later period larger.

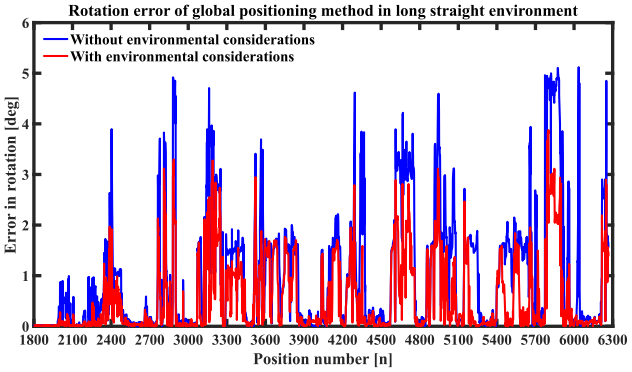

FIGURE 13. Rotation error of the MIT-Killian-Court. Although the error is oscillating, the overall error is higher without considering the environment.

narrow environments are easy to distinguish. As with the ACES-Building dataset, images before position number 1800 were omitted. As shown in Figs. 12 and 13, translation and rotation errors were particularly obvious in the stage of the experimental process.

In summary, the technique proposed in this article improved positioning accuracy in long straight environments. Translation errors that considered the influence of these environments were smaller than those that did not consider the environment. This approach also led to the suppression of rotation errors. A statistical analysis of the translation and rotation errors for the two datasets was determined using:

$$\frac{\sum_{i}^{n} P_i^{RSME}}{\sum_{i}^{n} Q_i^{RSME}} \times 100\% \tag{13}$$

where P_i^{RSME} and the Q_i^{RSME} represent represent the error values for models considering and not considering the influence of environmental characteristics, respectively.

As shown in Table 4, the average translation and rotation errors decreased by 27.29% and 25.82% respectively. These results indicate that considering the characteristics of long and straight environments leads to improved reliability.

TABLE 4. Statistics of Translation and Rotation Absolute Pose Errors of ACES-Building and MIT-Killian-Court Dataset .

Error types	ACES-Building	MIT-Killian-Court	Mean value
Translation error	23.22%	31.37%	27.29%
Rotation error	24.14%	27.49%	25.82%

TABLE 5. Comparison of ICP-based combined methods with CSM-based combined methods on ACES-Building and MIT-Killian-Court datasets.

Datasets	Methodology	Average output time of single pose	Average matching rate
ACES	ICP-based	3.281 ms	77.31%
	CSM-based	5.866 ms	95.53%
MIT	ICP-based	11.442 ms	63.42%
	CSM-based	17.272 ms	87.63%

As discussed above, ICP and RANSAC are two commonly used methods for scan matching and line fitting, respectively. In this study, these methods were combined and used for long straight corridor positioning. The combined algorithm was tested using the ACES-Building and MIT-Killian-Court datasets, as shown in Figure 14. Figures 14a and 14b show output results for each dataset, produced by combining CSM matching and weighted line fitting. Figures 14c and 14d show output results from ICP and RANSAC. The blue and green lines in the figure indicate pose trajectory outputs. The ICP algorithm alone is not suitable for large-scale scenarios, the results for these two datasets are particularly fragmented. In addition, the RANSAC algorithm is a non-deterministic model that produces reasonable results with certain probabilities, which are directly proportional to the number of iterations. And the RANSAC can only provide estimates in variable 2D environments. As such, judgment results in narrow corridors that are often unsatisfactory.

It is evident from the thumbnail images that the fusion algorithm based on CSM is more robust than that of ICP. The experimental data shown in Table 5 includes the average output time for a single pose, which refers to the ratio between the output time of all poses and the total number of poses. The average matching rate is the ratio between the sum of the matching rate of a single pose and the total number of poses. In small datasets, such as ACES-Building, the average output time for single poses is relatively small, suggesting the fusion algorithm based on ICP offers lower complexity. However, the result is not ideal as the match rate is too low, resulting in lower accuracy.

A different effect was observed in larger datasets, such as MIT-Killian-Court. In the experiment, we found the two fusion methods required additional iterations to output a pose when the dataset was in the final stage. However, the fusion method based on CSM offered a higher matching rate, especially for large turning angles.

C. TESTING IN REAL CORRIDORS

To evaluate the performance of our proposed algorithm, a series of physical experiments were conducted. The

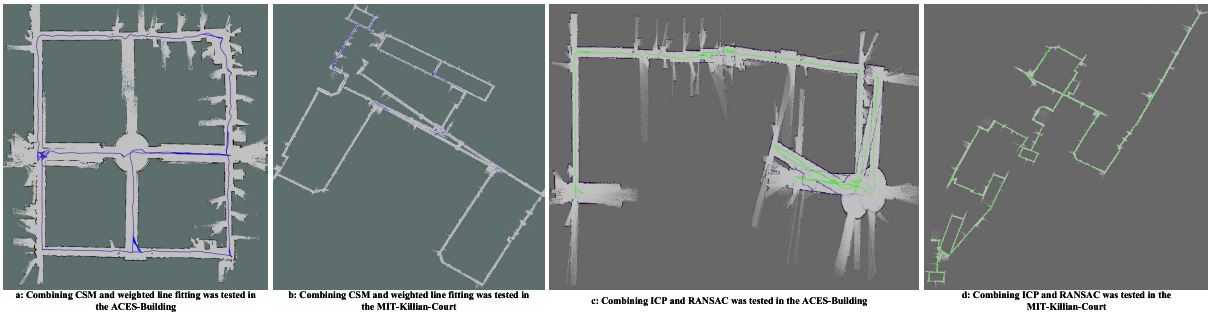

FIGURE 14. The performance of two different fusion algorithms on different datasets.

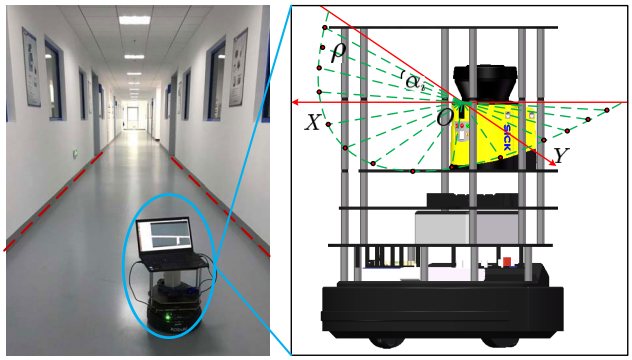

FIGURE 15. Actual corridor environment and experimental hardware configuration.The red dotted line represents the segment fitted in the corridor environment.

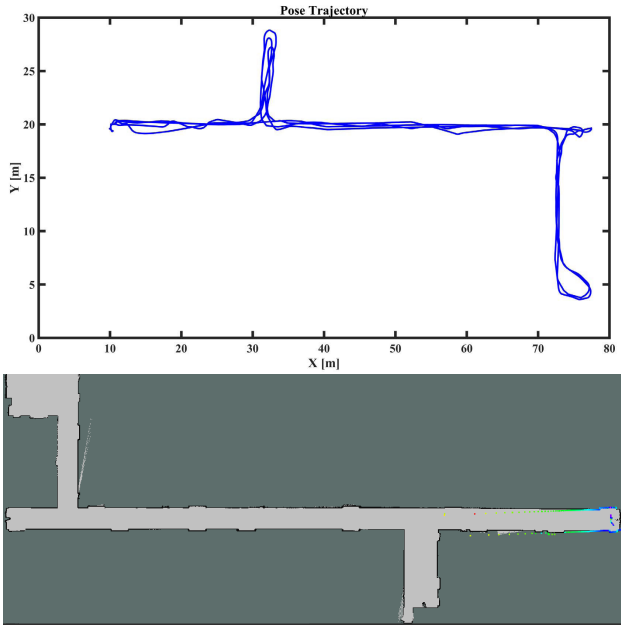

FIGURE 16. The pose trajectory and the constructed corridor map. this long straight corridor is about 70 meters long, the mobile robot made three turns in the environment.

effectiveness of the proposed algorithm in real environments was assessed using a mobile robot in a long straight corridor.

A real scenario using a long straight corridor was selected to test the proposed algorithm. The hardware system

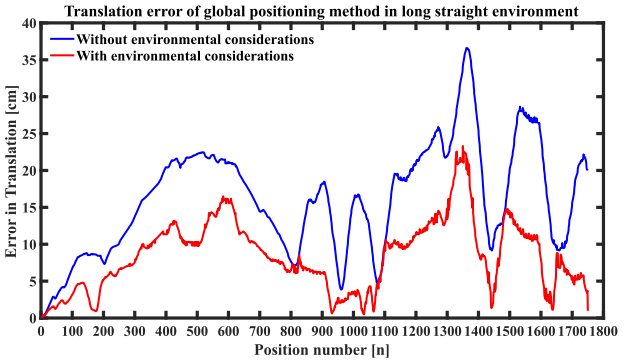

FIGURE 17. The translation pose error in the actual corridor environment.

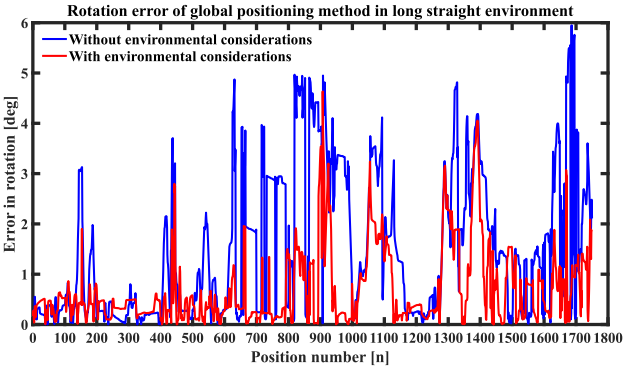

FIGURE 18. The rotation pose error in the actual corridor environment.

consisted of a laptop with an i7 processor and a TurtleBot2 mobile robot, equipped with SICK LMS111 lidar. This configuration is shown in Figure 15. A corridor with a length of 70 meters meters is shown in Figure 16. The hallway only contains doors, walls, and some fire-fighting equipment, which was suitable for testing the proposed algorithm.

The proposed global positioning algorithm was implemented using a TurtleBot2. The laser sensor was mounted on the mobile robot and the dataset from the corridor was acquired using manual operation. Figure 16 shows the pose trajectory and constructed map for the mobile robot in the actual environment.

Consistency was ensured by first collecting scanning information and then using global localization algorithms, both

with and without long straight parameter adjustments, to process the data. The resulting translation errors are shown in Figures 17 and 18.

Test results in the actual scene indicate that considering the influence of long straight environments results in lower translation and rotation errors. It can also be seen that the algorithm plays a positive role in the global localization of the narrow corridor.

V. CONCLUSION

This study proposed a novel global localization method for mobile robots in long and straight indoor environments, in which the global pose was adjusted for the first time by combining a weighted line fitting model with correlation scan matching. The prior environment was determined using a line extraction method. The linear fitting model was used to determine environmental characteristics and, in combination with correlation scan matching, output global posture weights.

Scan data in the narrow corridor were combined with internal sensor positions during correlation scan matching to update weight values. A validation experiment, conducted using public datasets and a physical environment, produced relatively low errors, thereby verifying the effectiveness of the proposed model.

REFERENCES

[1] C. Cadena, L. Carlone, H. Carrillo, Y. Latif, D. Scaramuzza, J. Neira, I. Reid, and J. J. Leonard, "Past, present, and future of simultaneous localization and mapping: Toward the robust-perception age," *IEEE Trans. Robot.*, vol. 32, no. 6, pp. 1309–1332, Dec. 2016.

[2] G. Bresson, Z. Alsayed, L. Yu, and S. Glaser, "Simultaneous localization and mapping: A survey of current trends in autonomous driving," *IEEE Trans. Intell. Vehicles*, vol. 2, no. 3, pp. 194–220, Sep. 2017.

[3] S. Huang and G. Dissanayake, "A critique of current developments in simultaneous localization and mapping," *Int. J. Adv. Robot. Syst.*, vol. 13, no. 5, Sep. 2016, Art. no. 172988141666948.

[4] A. Censi, "Scan matching in a probabilistic framework," in *Proc. IEEE Int. Conf. Robot. Autom.*, May 2006, pp. 2291–2296.

[5] S. Park, "Spectral scan matching for robot pose estimation," *Electron. Lett.*, vol. 45, no. 21, pp. 1076–1077, Dec. 2009.

[6] J. Rowekamper, C. Sprunk, G. D. Tipaldi, C. Stachniss, P. Pfaff, and W. Burgard, "On the position accuracy of mobile robot localization based on particle filters combined with scan matching," in *Proc. IEEE/RSJ Int. Conf. Intell. Robots Syst.*, Oct. 2012, pp. 3158–3164.

[7] Pomerleau, Franãois, Francis Colas, and Roland Siegwart, "A review of point cloud registration algorithms for mobile robotics," Tech. Rep., 2015.

[8] H. Kim, S. Song, and H. Myung, "GP-ICP: Ground plane ICP for mobile robots," *IEEE Access*, vol. 7, pp. 76599–76610, 2019.

[9] P. Biber and W. Strasser, "The normal distributions transform: A new approach to laser scan matching," in *Proc. IEEE/RSJ Int. Conf. Intell. Robots Syst. (IROS)*, 2003, pp. 2743–2748.

[10] T. Takubo, T. Kaminade, Y. Mae, K. Ohara, and T. Arai, "NDT scan matching method for high resolution grid map," in *Proc. IEEE/RSJ Int. Conf. Intell. Robots Syst.*, Oct. 2009, pp. 1517–1522.

[11] E. Olson, "M3RSM: Many-to-many multi-resolution scan matching," in *Proc. IEEE Int. Conf. Robot. Autom. (ICRA)*, May 2015, pp. 5815–5821.

[12] E. B. Olson, "Real-time correlative scan matching," in *Proc. IEEE Int. Conf. Robot. Autom.*, May 2009, pp. 4387–4393.

[13] J. Song, H. Gao, X. Zhang, W. Lin, and J. Liu, "A global localization algorithm for mobile robots based on grid submaps," in *Proc. 3rd Int. Conf. Adv. Robot. Mechatronics (ICARM)*, Jul. 2018, pp. 201–206.

[14] S.-H. Chan, P.-T. Wu, and L.-C. Fu, "Robust 2D indoor localization through laser SLAM and visual SLAM fusion," in *Proc. IEEE Int. Conf. Syst., Man, Cybern. (SMC)*, Oct. 2018, pp. 1263–1268.

[15] T. Oh, D. Lee, H. Kim, and H. Myung, "Graph structure-based simultaneous localization and mapping using a hybrid method of 2D laser scan and monocular camera image in environments with laser scan ambiguity," *Sensors*, vol. 15, no. 7, pp. 15830–15852, Jul. 2015.

[16] A. Schaefer, D. Buscher, L. Luft, and W. Burgard, "A maximum likelihood approach to extract polylines from 2-D laser range scans," in *Proc. IEEE/RSJ Int. Conf. Intell. Robots Syst. (IROS)*, Oct. 2018, pp. 4766–4773.

[17] Y. Chen, J. Tang, C. Jiang, L. Zhu, M. Lehtomäki, H. Kaartinen, R. Kaijaluoto, Y. Wang, J. Hyyppä, H. Hyyppä, H. Zhou, L. Pei, and R. Chen, "The accuracy comparison of three simultaneous localization and mapping (SLAM)-based indoor mapping technologies," *Sensors*, vol. 18, no. 10, p. 3228, Sep. 2018.

[18] R. Tiar, N. Ouadah, O. Azouaoui, M. Djehaich, H. Ziane, and N. Achour, "ICP-SLAM methods implementation on a bi-steerable mobile robot," in *Proc. IEEE 11th Int. Workshop Electron., Control, Meas., Signals their Appl. Mechatronics*, Jun. 2013, pp. 1–6.

[19] E. Mendes, P. Koch, and S. Lacroix, "ICP-based pose-graph SLAM," in *Proc. IEEE Int. Symp. Saf., Secur., Rescue Robot. (SSRR)*, Oct. 2016, pp. 195–200.

[20] J. Zhu, N. Zheng, and Z. Yuan, "An improved technique for robot global localization in indoor environments," *Int. J. Adv. Robot. Syst.*, vol. 8, no. 1, p. 7, Mar. 2011.

[21] A. Censi, "An ICP variant using a point-to-line metric," in *Proc. IEEE Int. Conf. Robot. Autom.*, May 2008, pp. 19–25.

[22] A. L. Pavlov, G. W. Ovchinnikov, D. Y. Derbyshev, D. Tsetserukou, and I. V. Oseledets, "AA-ICP: Iterative closest point with anderson acceleration," in *Proc. IEEE Int. Conf. Robot. Autom. (ICRA)*, May 2018, pp. 1–6.

[23] S. Bonnabel, M. Barczyk, and F. Goulette, "On the covariance of ICP-based scan-matching techniques," in *Proc. Amer. Control Conf. (ACC)*, Jul. 2016, pp. 5498–5503.

[24] J. Elseberg, S. Magnenat, R. Siegwart, and A. Nüchter, "Comparison of nearest-neighbor-search strategies and implementations for efficient shape registration," *J. Softw. Eng. Robot.*, vol. 3, no. 1, pp. 2–12, 2012.

[25] J. L. Li and Y. X. Sun, "Mapping of rescue environment based on NDT scan matching," *Adv. Mater. Res.*, vols. 760–762, pp. 928–933, Sep. 2013.

[26] Y. He, B. Zhou, X. Li, K. Qian, and X. Ma, "S4OM: A real-time lidar odometry and mapping system based on Super4PCS scan-matching," in *Proc. IEEE Int. Conf. Robot. Biomimetics (ROBIO)*, Dec. 2018, pp. 212–217.

[27] W. Hess, D. Kohler, H. Rapp, and D. Andor, "Real-time loop closure in 2D LIDAR SLAM," in *Proc. IEEE Int. Conf. Robot. Autom. (ICRA)*, May 2016, pp. 1271–1278.

[28] Sun, Yuxiang, Ming Liu, and Max Q-H. Meng, "WiFi signal strength-based robot indoor localization," in *Proc. IEEE Int. Conf. Inf. Automat. (ICIA)*, 2014, pp. 250–256.

[29] A. Codas, M. Devy, and C. Lemaire, "Robot localization algorithm using odometry and RFID technology," *IFAC Proc. Volumes*, vol. 43, no. 16, pp. 569–574, 2010.

[30] M. Brossard and S. Bonnabel, "Learning wheel odometry and IMU errors for localization," in *Proc. Int. Conf. Robot. Autom. (ICRA)*, May 2019, pp. 291–297.

[31] G. A. Borges and M.-J. Aldon, "A split-and-merge segmentation algorithm for line extraction in 2D range images," in *Proc. 15th Int. Conf. Pattern Recognit.*, 2000, pp. 441–444.

[32] L. Zhang and B. K. Ghosh, "Line segment based map building and localization using 2D laser rangefinder," in *Proc. IEEE Int. Conf. Robot. Automat. Symp. Process.*, 2000, pp. 2538–2543.

[33] H. Gao, X. Zhang, Y. Fang, and J. Yuan, "A line segment extraction algorithm using laser data based on seeded region growing," *Int. J. Adv. Robotic Syst.*, vol. 15, no. 1, Jan. 2018, Art. no. 172988141875524.

[34] Y. Sun, M. Liu, and M. Q.-H. Meng, "Improving RGB-D SLAM in dynamic environments: A motion removal approach," *Robot. Auto. Syst.*, vol. 89, pp. 110–122, Mar. 2017.

[35] M. A. Fischler and R. Bolles, "Random sample consensus: A paradigm for model fitting with applications to image analysis and automated cartography," *Commun. ACM*, vol. 24, no. 6, pp. 381–395, 1981.

[36] S. T. Pfister, S. I. Roumeliotis, and J. W. Burdick, "Weighted line fitting algorithms for mobile robot map building and efficient data representation," in *Proc. IEEE Int. Conf. Robot. Autom.*, Sep. 2003, pp. 1304–1311.

[37] Y. Sun, M. Liu, and M. Q.-H. Meng, "Motion removal for reliable RGB-D SLAM in dynamic environments," *Robot. Auto. Syst.*, vol. 108, pp. 115–128, Oct. 2018.

[38] G. Grisetti, C. Stachniss, and W. Burgard, "Improved techniques for grid mapping with rao-blackwellized particle filters," *IEEE Trans. Robot.*, vol. 23, no. 1, pp. 34–46, Feb. 2007.
[39] R. Kāmmerle, "On measuring the accuracy of SLAM algorithms," *Autonomous Robot.*, vol. 27, no. 4, p. 387, 2009.
[40] K. Krinkin, A. Filatov, A. Y. Filatov, A. Huletski, and D. Kartashov, "Evaluation of modern laser based indoor SLAM algorithms," in *Proc. 22nd Conf. Open Innov. Assoc. (FRUCT)*, May 2018.
[41] A. Filatov, A. Filatov, K. Krinkin, B. Chen, and D. Molodan, "2D SLAM quality evaluation methods," in *Proc. 21st Conf. Open Innov. Assoc. (FRUCT)*, Nov. 2017, pp. 120–126.
[42] H. Li, Q. Zhang, and D. Zhao, "Comparison of methods to efficient graph SLAM under general optimization framework," in *Proc. 32nd Youth Academic Annu. Conf. Chin. Assoc. Autom. (YAC)*, May 2017, pp. 321–326.
[43] Bonarini, Andrea, "Rawseeds: Robotics advancement through Web-publishing of sensorial and elaborated extensive data sets," in *Proc. IROS*. vol. 6, 2006, p. 93.

LINGDONG ZENG (Graduate Student Member, IEEE) received the M.S. degree in electronics and communications engineering from Northwest Normal University, Lanzhou, China, in 2018. He is currently pursuing the Ph.D. degree with the School of Mechatronic Engineering and Automation, Shanghai University. His research focuses are simultaneous localization and mapping, large-scale map generation, and robot navigation.

SHUAI GUO received the Ph.D. degree in mechanic engineering and automation from Shanghai University, Shanghai, China, in 2006. He is currently a Professor with Shanghai University and the Vice President of the Shanghai Robot Industry Technology Research Institute. His research interests include robotics, rehabilitation robot, and industrial robot.

ZHEN XU received the B.S. degree in mechanical design, manufacturing, and automation from Dezhou University in 2014 and the M.S. degree in mechanical engineering from the University of South China in 2017. He is currently pursuing the Ph.D. degree with the School of Mechatronic Engineering and Automation, Shanghai University. He has been engaged in research fields of robot design and navigation and simultaneous localization and mapping since 2014. He is a Student Member of the Shanghai Robotics Society.

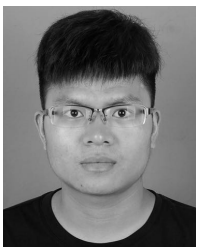

MENGMENG ZHU received the B.S. degree in process equipment and control engineering from the Inner Mongolia University of Science and Technology, Baotou, China, in 2018. He is currently pursuing the M.S. degree in mechanical engineering from Shanghai University. His research interests include mobile robot navigation.